LC GC
north america
solutions for separation scientists

Characterization of Hyaluronic Acid with On-Line Differential Viscometry, Multiangle Light Scattering, and Differential Refractometry

Hyaluronic acid (HA) is a naturally occurring, unbranched polysaccharide that consists of alternately repeating D-glucuronic acid and *N*-acetylglucosamine units. This biopolymer is present throughout all mammalian systems but occurs primarily in synovial (joint) fluid, vitreous humor, and various loose connective tissues (such as rooster comb) (1). HA is of enormous commercial interest for ophthalmic, medical, pharmacological, and cosmetic applications.

Jason Waters* and Danielle Leiske†
*Wyatt Technology Corporation, Santa Barbara, California, e-mail jwaters@wyatt.com
†Department of Chemical Engineering, Oregon State University, Corvallis, Oregon.

Address correspondence to J. Waters.

Hyaluronic acid (HA) has been studied extensively by many groups in the past (1–7). The physiochemical behavior of HA has been tied closely to material characteristics such as the weight-average molecular weight (M_w), molecular weight distribution (also known as polydispersity index [PDI]), intrinsic viscosity ([η]), and molecular conformation.

Past studies of HA have included many size-exclusion chromatography (SEC) experiments. Traditional SEC involves chromatographically separating samples and monitoring the output with a concentration detector such as a refractometer or UV absorbance detector. SEC in this form is a purely relative measurement, because the chromatographic system must first be calibrated with a series of known M_w standards, collectively known as a calibration curve. Other SEC studies of HA have added multiangle light-scattering (MALS) devices in series with concentration detectors. This proves advantageous because MALS is an extremely sensitive technique for measuring absolute M_w, as it does not rely on calibration standards or a priori assumptions about the molecular conformation. One also can determine a sample's root mean-square radius (erroneously, but frequently referred to as the radius of gyration), R_g, by using a MALS instrument, provided the sample R_g is greater than about 10 nm.

The Mendichi group at the Istituto di Chimica delle Macromolecole (Milan, Italy) has performed a number of elegant experiments involving on-line SEC of HA utilizing MALS, concentration detection, and single-capillary viscometry (2,3). This combination of detectors yields not only all of the aforementioned material characteristics but also elucidates sample intrinsic viscosity and, using the Mark–Houwink–Sakurada (MHS) relationship, molecular conformation information. Single-capillary viscometry is inherently vulnerable to noise generated by system pressure fluctuations. The pressure associated with laminar fluid flow through capillaries is first order with respect to flow rate, as can be seen in Poiselle's law

$$Q = \Delta p / R\eta \qquad [1]$$

where Q is mass flow rate, Δp is the pres-

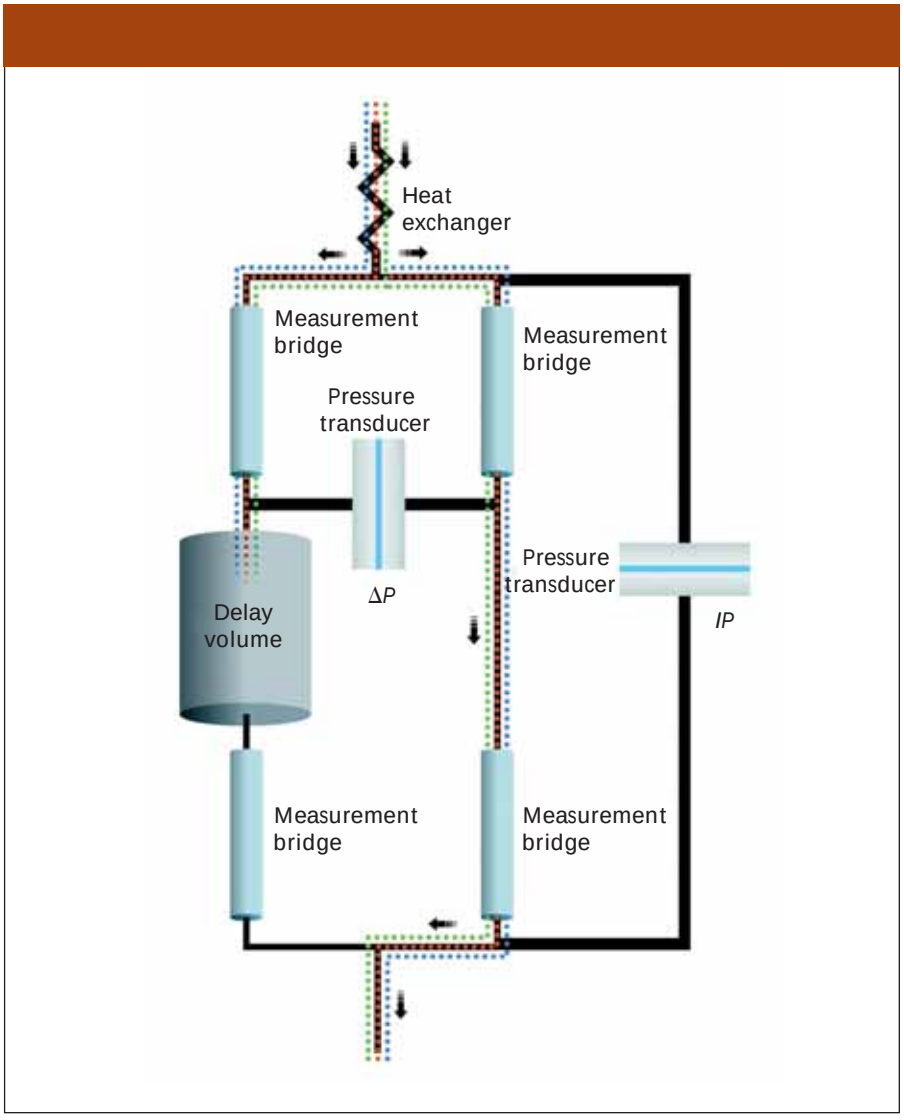

Figure 1: Schematic of the differential viscometer design.

sure drop across the capillary, R is the flow impedance through the capillary, and η is the fluid viscosity.

This means that even slight changes in flow rate can lead to vastly increased baseline noise. Such flow rate fluctuations are virtually omnipresent in commercial chromatography pumps in the form of pump pulsations. Increased baseline noise leads to a lower signal-to-noise ratio (S/N) and thus lowered experimental accuracy. Using elaborate pulse dampeners, pump pulses can be reduced but, unfortunately, not eliminated. Even using a pulse-free pump and Fourier-transform data filtering, single-capillary viscometry detector S/N of only approximately 125:1 has been shown (8,9). Another drawback of this technique is its reliance on universal calibration. Before use, the single-capillary viscometry device must first be calibrated using a large number of known standards.

This article discusses on-line absolute characterization of HA properties using MALS, differential refractometry, and differential viscometry detectors in series. Utilizing differential viscometry is particularly advantageous as compared with single-capillary viscometry, as will be shown.

Table I: Summary of HA sample material characteristics

HA Sample	HA Source	M_W (g/mol)	PDI	R_g (nm)	[η] (mL/g)	r_h (nm)
HA-1	Bacterial fermentation	2.64E+05	1.19	57.7	632	27.7
HA-2	Umbilical cord	2.84E+05	1.23	66.1	652	28.3
HA-3	Chicken comb	6.62E+05	1.10	109.1	1431	51.1
HA-4	Bacterial fermentation	1.10E+06	1.45	165.4	1754	57.7
HA-5	Umbilical cord	1.44E+06	1.06	180.4	2208	77.7
HA-6	Chicken comb	1.62E+06	1.06	182.4	2671	86.1
HA-7	"Natural sources"	1.76E+06	1.02	207.9	2655	89.9

Materials and Methods

Seven separate HA samples were used for this study. Sample root sources varied, and included HA from rooster comb, umbilical cord, and bacterial fermentation. Ovalbumin was obtained from Sigma (St. Louis, Missouri). All other chemicals were analytical grade.

The chromatographic system consisted of an HPLC system and autoinjector (Agilent 1100 [Agilent Technologies, Wilmington, Delaware], 900-µL injection loop), including a solvent degasser (ERC L761). The SEC column system consisted of a Polymer Labs (Amherst, Massachusetts) Aquagel - OH (8 µm) separation column with guard column. The mobile phase was phosphate-buffered saline (PBS, 8 mM dibasic sodium phosphate, 22 mM monobasic sodium phosphate, 150 mM sodium chloride in MilliQ-grade water). The flow rate was 0.5 mL/min. Chromatographic detectors included a DAWN EOS MALS device, a ViscoStar differential viscometer, and an Optilab rEX differential diffractometer in series (all from Wyatt Technology, Santa Barbara, California).

The MALS detector enables calculation of the absolute molar mass without the need for reference standards, column calibration, or "fudge factors."

The differential viscometer uses the traditional four-arm capillary bridge design (Figure 1).

The bridge is composed of four equal-impedance capillaries with the lower-left arm possessing an effectively zero-impedance delay volume. As mobile phase propagates through the device, the differential pressure (ΔP) transducer in the center of the bridge reads zero. When the sample enters the bridge, it splits evenly. When the sample

$$\eta_{sp} = \eta/\eta_0 - 1 = \frac{4\Delta P}{(IP - 2\Delta P)} \qquad [2]$$

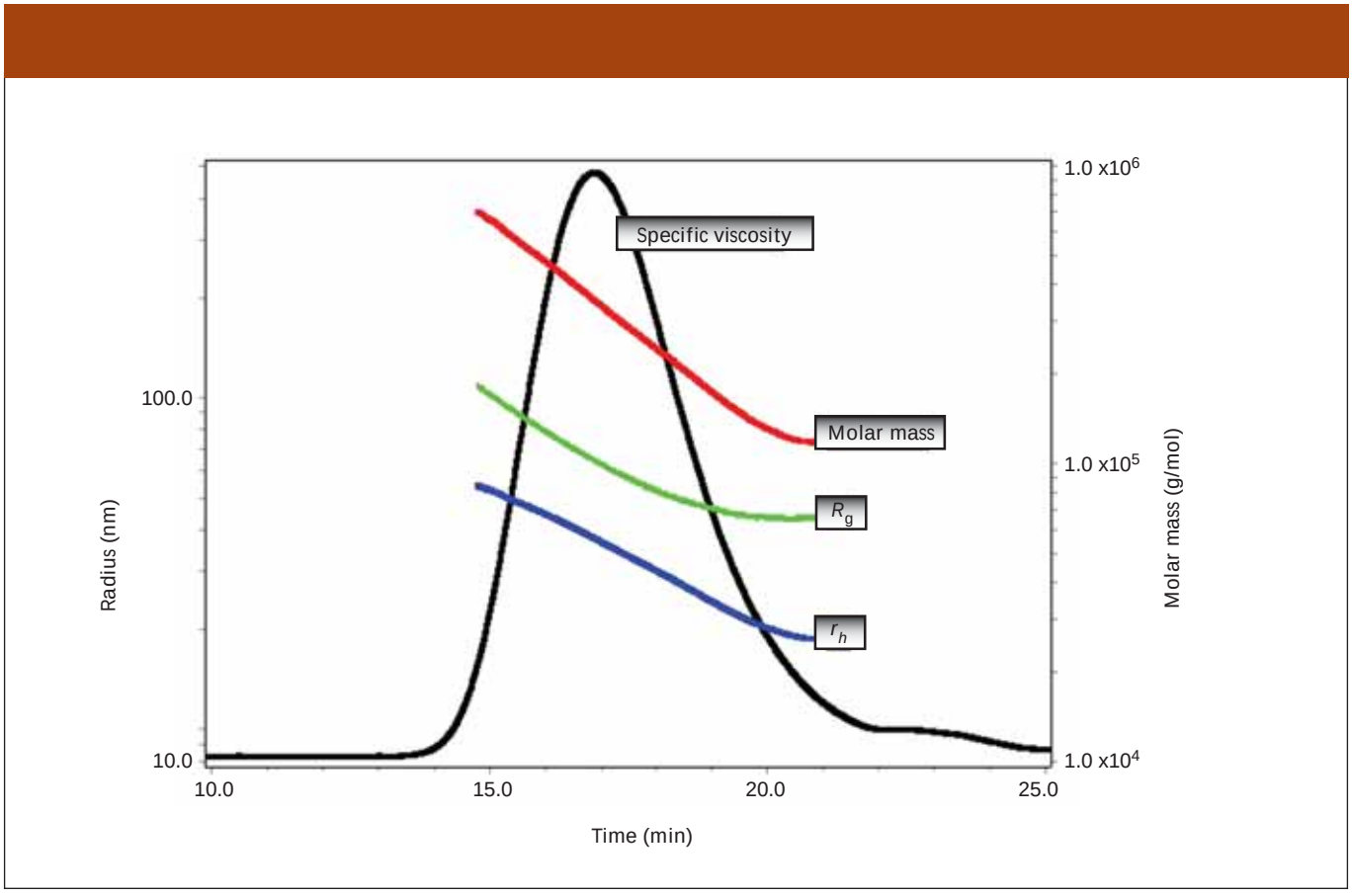

Figure 2: η_{sp} chromatogram of sample HA-2 with associated M_w, R_g, and r_h values across the peak.

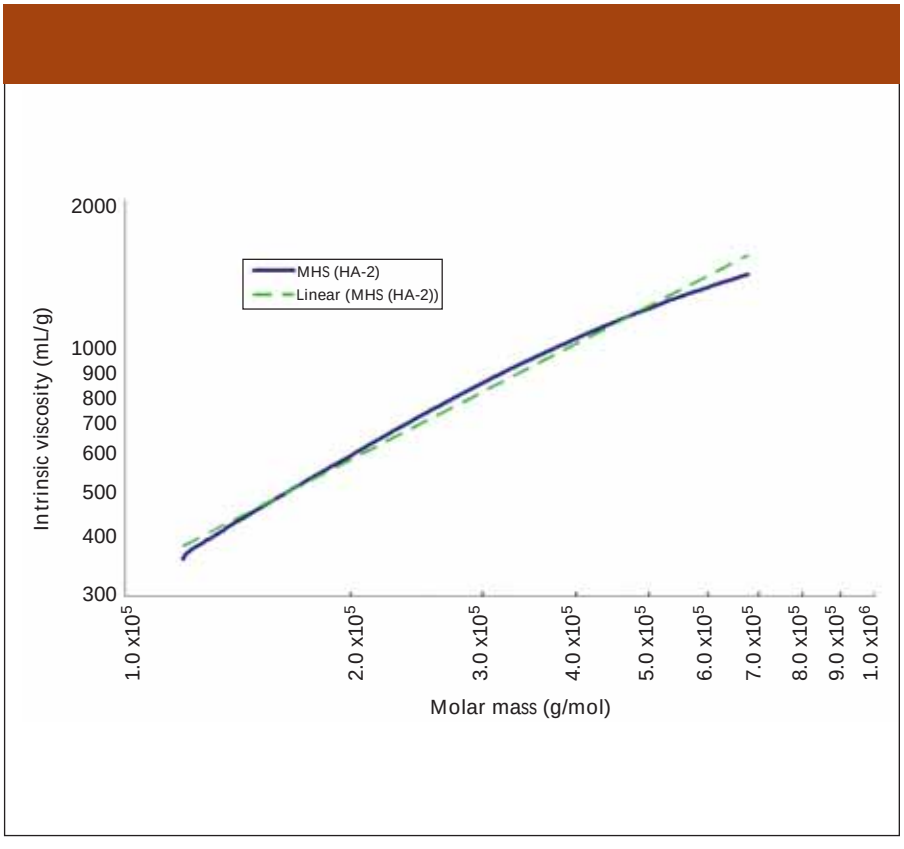

Figure 3: Mark–Houwink–Sakurada plot and linear fit for sample HA-2.

enters the delay volume, three capillaries contain sample and one contains only mobile phase. This creates a pressure imbalance within the bridge that is detected by ΔP. The sample specific viscosity (η_{sp}) can be directly determined from the combination of this ΔP pressure imbalance and the device inlet pressure (IP) by means of the following relationship as derived from the Stokes–Einstein equation (10)

where η is the sample viscosity and η_o the solvent viscosity.

This is a direct measurement that depends only upon calibrated pressure transducers. The bridge design is inherently insensitive to pressure fluctuations and thus is able to tolerate moderate pump pulses. Additionally, the device utilizes a Peltier thermoelectric device for precision thermal control within a large temperature range, including at or

$$[\eta] = \lim_{c \to 0} \eta_{sp} / c \qquad [3]$$

below room temperature. The combination of bridge design, precise thermal control, and contemporary electronics results in a

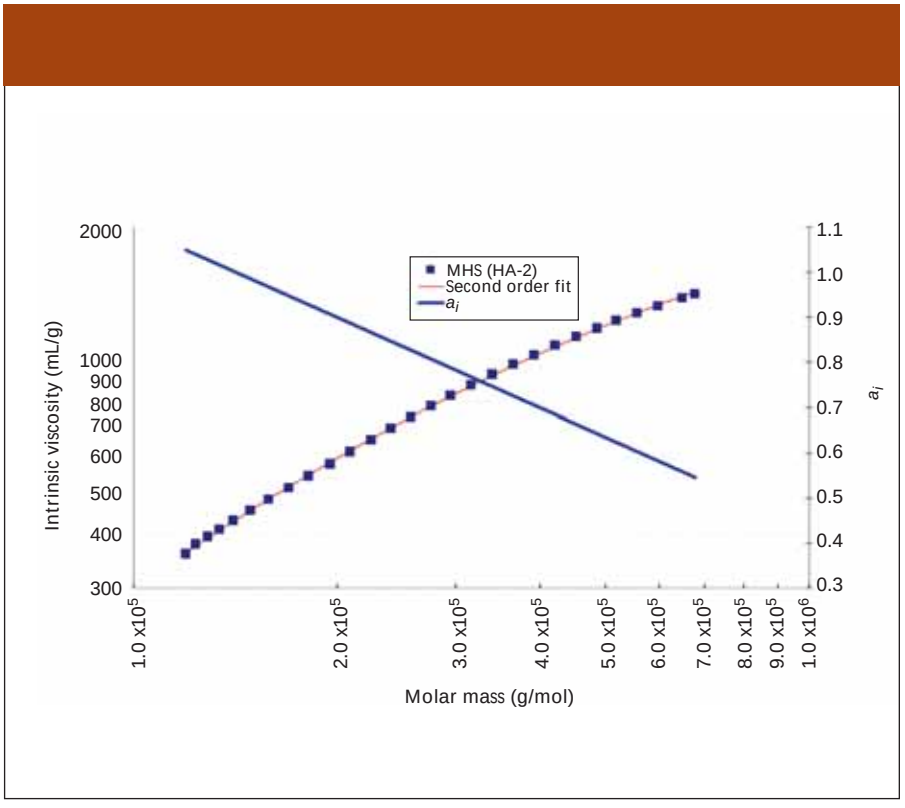

Figure 4: Mark–Houwink–Sakurada plot, second-order fit, and a_i versus log(M_W) for sample HA-2.

device with outstanding S/N.

The differential refractometer was used for concentration measurements. Thermal control via a Peltier device allows for thermal stability at or below room temperature, and thus stable baselines and extremely high S/N.

Knowledge of both η_{sp} as determined by the differential viscometer and concentration c as determined by the differential refractometer allow for the direct calculations of sample intrinsic viscosity [η] by applying the following relationship to every data slice across an elution peak

By including a light-scattering device, the data can be fit to the MHS equation. The MHS relationship is

$$[\eta] = KM^a \quad [4]$$

where M is molecular weight and both K and a are MHS coefficients. These MHS coefficients are measures of polymer shape and solvent interaction. The a value in particular is an indicator of polymer shape in solution, with lower a values (for example, $a < 0.5$), indicating more compact conformations and higher a (for example, $a > 0.8$) values, indicating extended conformations.

The hydrodynamic volume V_h of the sample also can be determined by means of the Einstein–Simha relation:

$$V_h = M[\eta]/(2.5N_A) \quad [5]$$

HA molecular conformation, as elucidated by MHS analysis, has been found to exhibit unusual behavior, as shown previously by the Mendichi group.

where N_A is Avogadro's number.

From this, one can derive the hydrodynamic radius r_h as

$$r_h = (3V_h/4\pi)^{1/3} \quad [6]$$

Defined this way, r_h is the radius of a sphere that has the same [η] as the sample.

Experimental collection and data analysis were performed with the ASTRA V software package (Wyatt Technology). Using this software, we were able to collect and subsequently analyze all 18 MALS angles along with the ΔP, IP, and differential refractometry signals. The software utilizes a proprietary band-broadening correction algorithm, which solves the long-standing problem of interdetector band broadening.

As the sample travels through the detectors, each flow cell acts like a small mixing volume. These discrete mixing chambers cause an initially sharp peak to broaden with a slight exponential tail. Left uncorrected, this causes experimental results to be slightly distorted (10). Band broadening is a function of all chromatography experiments. It is present whenever more than one detector is used for HPLC detection.

Results and Discussion

Before performing HA chromatographic analysis, the exact system constants specific to our experimental setup needed to be determined. It should be noted that placement of the differential viscometer upstream of the differential refractometer is necessary, as differential refractometer baseline behavior is sensitive to backpressure effects. Thus, for the best S/N, the refractometer should be the last detector in the chromatographic flow path. As a side effect (because of the sample split across the differential viscometer's bridge), the refractometer only sees effectively half of the injected sample mass during initial peak elution. The software utilizes a factory-set dilution factor for the differential viscometer to adjust for this.

Please see Table I for a summary of material characteristics for the seven HA samples. All solution concentrations were 0.1 mg/mL HA in PBS. The injection volume was 900 mL. The dn/dc value for HA, 0.167 (mL/g), was taken from the literature (1). The low concentration and large injected volume were selected to avoid potential viscous-fingering of HA samples within the separation column. Results are in agreement with published values (1–3,5). Injections were performed multiple times for each sample to verify repeatability of results.

Figure 2 shows a typical η_{sp} chromatogram of an HA sample along with the associated M_w, R_g, and r_h values across the peak. The typical differential viscometer S/N of the η_{sp} trace for these HA experiments was on the order of 2200:1, more than one order of magnitude better than pulse-free, data-filtered single-capillary viscometry.

To evaluate molecular conformation information, MHS plots have been constructed for all samples. See Figure 3 for a representative

MHS plot of sample HA-2.

The least-squares regression of the MHS trace also can be seen in Figure 3. From this regression, the K and a values for sample HA-2 can be calculated as $K = 0.0277$ and $a = 0.817$, both values being close to published values. However, these numbers should not be taken at face-value, as it can be seen that the MHS trace shows marked curvature. Though not shown, all seven HA samples tested within this study exhibited MHS curvature similar to that seen in Figure 3. Because all HA MHS plots show curvature, the K and a coefficients as determined by direct linear regression of MHS plots cannot be taken as accurate descriptors of MHS behavior across the entire gamut of HA molecular weights. Indeed, this is true of previously published K and a values.

By using a polynomial fit (in this case second order) of the MHS curve and subsequently taking the derivative of that function, one can determine instantaneous $a(a_i)$ values. That is

$$a_i = d(\log[\eta])/d(\log[M]) \quad [7]$$

See Figure 4 for the a_i values of sample HA-2. a_i values for this particular sample range from 1.0 at lower molecular weights decreasing to nearly 0.55 at high molecular weights. The six other HA samples showed a_i behavior analogous to that described earlier, with typical a_i values ranging from 1.1 at low molecular weights to 0.5 at high molecular weights.

This behavior has been attributed to the theory that HA exhibits free-draining, non-Gaussian chain behavior at lower molecular weights (2). The inherent stiffness of this polyelectrolyte forces the molecule to take on a more extended conformation at lower molecular weights, and thus a correspondingly high a_i value. As molecular weight increases, HA slowly transitions into Gaussian chain behavior and a_i values drop. This might help explain the wide variety (and inconsistency) of HA MHS constants that have been published in the literature.

Conclusions

By combining a MALS instrument, a differential refractometer, and a differential viscometer with SEC, we have explored the material characteristics of the biopolymer HA. We have determined the absolute HA molecular weight, molecular weight distribution, and radii information to be consistent with historical literature values. HA molecular conformation, as elucidated by MHS analysis, has been found to exhibit unusual behavior, as shown previously by the Mendichi group. Utilization of these detectors in tandem with the software ensured rapid, accurate, absolute analysis of this behavior with unprecedented S/N and no need for calibration curves for any of the detectors.

References

(1) S. Hokputsa, J. Kornelia, C. Alexander, and S. Harding, Eur. Biophys. J. 32, 450–496 (2003).

(2) R. Mendichi, L. Soltes, and A. Giacometti Schieroni, Biomacromolecules 4, 1805–1810 (2003).

(3) R. Mendichi and A. Giacometti Schieroni, Polymer 43, 6115–6121.

(4) R. Mendichi, A. Giacometti Schieroni, C. Grassi, and A. Re, Polymer 39, 6611–6620 (1998).

(5) L. Soltes, R. Mendichi, D. Lath, M. Mach, and D. Bakos, Biomed. Chromatogr. 16, 459–462 (2002).

(6) K. Kazuaki, M. Kinoshita, and S. Yasueda, J. Chromatogr., B 797, 347–355 (2003).

(7) N. Berriaud, M. Milas, and M. Rinaudo , Int. J. Biol. Macromolecules 16, 137–142 (1994).

(8) R. Mendichi and A. Giacometti Schieroni, J. Appl. Polymer Sci. 68, 1651–1659 (1998).

Jason Waters is with Wyatt Technology Corporation, Santa Barbara, California.

Danielle Leiske is with Department of Chemical Engineering, Oregon State University, Corvallis, Oregon. ■